

Dielectric investigation of cold crystallization of poly(3-hydroxybutyrate)

Gamal R. Saad*, Ashraf A. Mansour and Amany H. Hamed

Chemistry Department, Faculty of Science, Cairo University, Orman-Giza, 12613, Egypt

(Revised 17 October 1996)

The dielectric behaviour of poly(3-hydroxybutyrate) (PHB) has been investigated for the glass (α) relaxation in the temperature and frequency ranges of -60 to 100°C and 10^3 – 10^5 Hz, respectively. Also, the crystallization kinetics of PHB has been studied dielectrically as a function of heating rate, time and temperature. Crystallinity has a marked influence on the glass relaxation characteristics owing to the relative constraint imposed on the amorphous phase by the crystallites. Furthermore, the results obtained showed that: (1) the optimum crystallization temperature is about 25°C ; (2) the time at which crystallization starts is a function of the working temperatures and apparently is reduced to just a few minutes at 40°C ; and (3) the crystallization process is completed within a period of less than 1 h in the temperature range 20 – 40°C . The bulk crystallization phenomena could be also described by the Avrami equation with an exponent ~ 3.8 .
© 1997 Elsevier Science Ltd.

(Keywords: dielectric measurements; poly(3-hydroxybutyrate); crystallization)

INTRODUCTION

Recently, much effort has been expended to find polymeric materials that can replace many synthetic materials and can degrade fully into harmless, naturally occurring small molecules¹. In this respect, intensive fundamental and applied research has been devoted to the study of the physical properties of poly(3-hydroxybutyrate) (PHB), and its related alkananoate^{2–14}, which are naturally occurring polymers produced by a wide variety of bacteria.

PHB is a highly crystalline thermoplastic polymer which is suitable for injection moulding and extrusion. In addition, it shows gas barrier properties comparable to those of poly(vinyl chloride) and poly(ethylene terephthalate). The combination of these properties may enable PHB to compete with commodity polymers in the packaging industries, especially in areas where non-biodegradable plastic items are not allowed due to environmental pollution¹⁵. A special property of PHB is the formation of large spherulites, which is probably due to its exceptional purity. For this reason, PHB has been studied as a model of spontaneous polymeric nucleation and crystallization, as it is free from any catalyst residues that are typically used in synthesis of polyolefins¹⁶. Previous studies of PHB showed that crystallization takes place from the melt over a wide range of temperatures including room temperature¹⁷. Remarkable embrittlement of PHB is observed at ambient temperatures, which is attributed to progressive crystallization occurring upon storage of the material. PHB can be rejuvenated by simple annealing treatment, preventing to a large extent subsequent ageing¹⁸.

Dielectric spectroscopy is a powerful technique that can detect the molecular dynamics as well as the

transformation phenomena in polymers at the earlier stages. A part of our present work is the study of dielectric relaxation of amorphous and highly crystalline PHB. We have also monitored the crystallization kinetics of PHB around room temperature dielectrically. In addition, d.s.c. was carried out to trace the crystallization behaviour.

EXPERIMENTAL

A commercial sample of bacterial origin of PHB was kindly supplied by Aldrich, USA.

Calorimetric measurements were carried out using a differential scanning calorimeter (PL-DSC) of Polymer Laboratories, UK. The calorimeter was calibrated for temperature, heat and heat flow according to the method recommended by GEFTA, Germany^{19,20}. The calorimetric measurements were carried out for small samples (3–5 mg) placed in sealed aluminium pans. The pans were heated at 200°C for 3 min, and the melt formed was then quenched rapidly in liquid nitrogen. D.s.c. measurements were carried out on the melt-quenched sample once immediately, and another after the elapse of 3 days at room temperature. The scans were carried out in the temperature range -60 to 200°C with heating rates of 10 and $20^\circ\text{C min}^{-1}$. The glass temperature, T_g , was taken as the inflection point of the specific heat increment, and the melting point, T_m , as the peak temperature of the melting endotherm. In contrast, when multiple endotherms were obtained, the temperature of the main peak was considered, and the enthalpy of fusion, ΔH_f , was directly obtained from the area under peaks.

Dielectric measurements were performed using a Polymer Laboratories dielectric thermal analyser (PL-DETA), which gives directly the dielectric constant, ϵ' , and loss, ϵ'' . Three types of measurements were undertaken: (1) temperature scans at a constant heating rate at

* To whom correspondence should be addressed

various frequencies; (2) temperature scans at different heating rates at constant frequency (10 kHz); and (3) isothermal measurements over extended periods of time at 10 kHz. The crystallization kinetics was monitored dielectrically using thin amorphous PHB films, which were obtained by pressing the PHB powder between two copper electrodes at 185°C for 5 min to obtain a condenser, which was also quenched in liquid nitrogen. This temperature/time regime was strictly followed for all samples in order to eliminate the nucleation contribution to the crystallization process and, therefore, confining the investigation only to the crystal growth process.

The crystallization process in the melt-quenched samples of PHB taking place at various temperatures, namely between 10 and 40°C, was traced dielectrically by measuring the dielectric constant at 10 kHz as a function of time over a period of 4 h at each temperature. This chosen frequency allows the three types of polarization to occur. It may be noted that the time elapsed between the removal of the sample from liquid nitrogen and the start of measurements was minimized to be less than 2 min. This was accomplished by adjusting the temperature of the dielectric measuring cell while it was empty to the required working temperature. Then, the sample was immediately inserted so that the time for attainment of thermal equilibrium was reduced, and, in turn, the possibility of any crystallization of the melt-quenched sample before the beginning of measurement also minimized.

The error in ϵ' and ϵ'' resulting from the change in the thickness associated with the crystallization is estimated to be less than 3.5%. This value is calculated from the densities of the crystalline and amorphous PHB (1.260 and 1.177 g cm⁻³, respectively)^{17,21} and by assuming that the final crystallization was about 56%.

RESULTS AND DISCUSSION

The d.s.c. scan of the melt-quenched PHB sample shows, as can be seen from Figure 1, a glass transition in the vicinity of -2°C, which is first followed by an exothermic crystallization peak at 45°C and then by a multiple of melting endotherms between 110 and 160°C. In contrast, repeated measurements of the same sample after 3 days show only multiple melting endotherms, and neither a glass transition nor an exothermic crystallization peak could be detected (see Figure 1). This

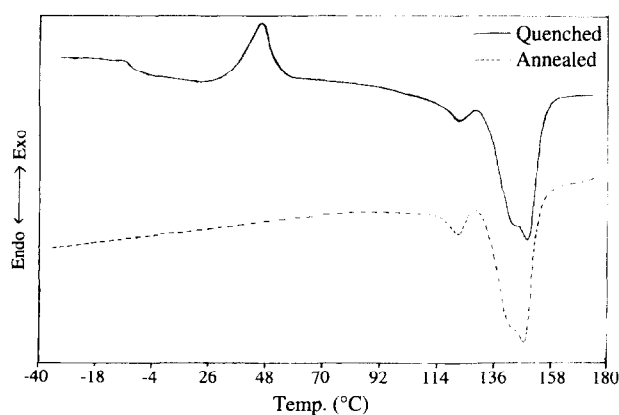


Figure 1 D.s.c. curves for PHB at a heating rate of 20°C min⁻¹: solid line, amorphous sample; broken line, annealed sample

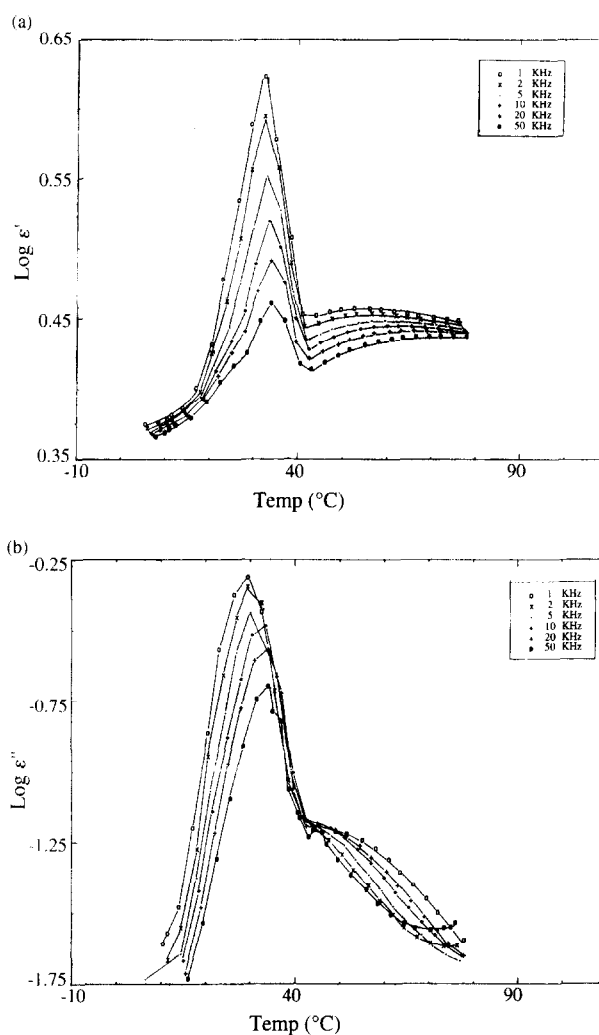


Figure 2 Temperature dependencies of (a) dielectric constant, ϵ' , and (b) dielectric loss, ϵ'' , at various frequencies for amorphous PHB

suggests that, most likely, the equilibrium crystallinity stage has already been attained.

A comparison between ΔH_f of a 100% crystalline sample, which is equal to 146 J g⁻¹¹⁷, with the measured value, which is equal to 73.2 J g⁻¹, implies the equilibrium crystallinity of our PHB sample amounts to $\sim 56 \pm 4\%$. This value is practically the same as that of the as-received PHB powder.

The temperature dependencies of the dielectric constant ϵ' , and the dielectric loss ϵ'' , at various frequencies for the amorphous PHB (the melt-quenched sample) are represented in Figure 2. The value of ϵ' in Figure 2a, increases sharply with increasing temperature, reaching a maximum at about 30°C. This increase corresponds to the dispersion of the α process in the amorphous phase of PHB, which is attributed to the micro-Brownian cooperative reorientation of the polymer segments associated with the glass transition. At temperatures above 30°C, the crystallization of the amorphous PHB starts and, in turn, results in a sudden decrease in ϵ' . The shape of the ϵ' curve above the maximum is determined by three factors: (1) temperature, which causes an increase in the number of reorienting dipoles; (2) the conversion of amorphous to crystalline material, therefore leading to a decrease in ϵ' ; and (3) the decrease in film thickness. From the known densities of the crystalline (1.260 g cm⁻³) and amorphous phases (1.177 g cm⁻³), the thickness

change is too small where it is expected to be less than 4%, assuming that the equilibrium crystallinity is about $56 \pm 4\%$. The thickness change affects only the dielectric constant above 30°C .

The ϵ'' , shown in Figure 2b, is similarly affected by the crystallization. First the amorphous sample undergoes a glass-rubber relaxation, α_b (the subscript b indicates 'before crystallization'), and ϵ'' shows a maximum. Then, ϵ'' decreases strongly due to crystallization, and an additional shoulder appears on the high-temperature side of the glass relaxation.

During cold crystallization, spherulites grow into the matrix until they impinge on each other. The spherulites consist of crystalline lamellae and constrained amorphous interlayers. The rigid amorphous fraction differs in electric field response from the normal amorphous phase. Thus, the molecular motion in the disordered (rigid amorphous) regions within the spherulites differs from that in the normal amorphous phase. This means that the second relaxation which appears as a shoulder on the high-temperature side of the α_b relaxation may be attributed to the micro-Brownian motion of chain segments of the rigid amorphous fraction in the crystalline regions. We call this process α_a , where the subscript a indicates 'after crystallization'.

Figure 3 represents the results for the same sample after cooling and annealing at room temperature for 3 days. A comparison between Figures 2 and 3 reveals the following characteristics. Firstly, the semicrystalline sample exhibits only the α_a relaxation process. Secondly, the α_a absorption band is much broader than that of the α_b peak, and the maximum in ϵ'' appears at higher temperatures (lower frequencies) than the maximum of the α_a peak. The logarithm of the measured frequencies is plotted against the corresponding reciprocal of the temperature at loss maximum, T_{max} , for the process of the annealed PHB sample. The experimental data, shown in Figure 4, can be fitted by the Meander equation²²⁻²⁴,

$$f_m = (f_0/\pi) e^{-Q_\gamma/RT} [1 - (1 - e^{\epsilon_s/RT})^{3r/d}]^{3(3r/d)^2(d/s)} \quad (1)$$

where f_0 is the local vibration frequency, Q_γ is local activation energy, $3r/d$ is the number of chain stems per structural unit, ϵ_s is the dislocation energy per segment, d is the interchain distance and s is the segment length. The fitting is carried out for Q_γ , $3r/d$ and ϵ_s , where f_0 , d , and s are given as known parameters and equal to 10^{13} Hz, 6.2 \AA and 4.1 \AA , respectively. The values obtained for Q_γ , ϵ_s and $3r/d$ are $30.18 \text{ kJ mol}^{-1}$, $4.115 \text{ kJ mol}^{-1}$ and 21.2 , respectively. The overlapping of the relaxation and crystallization processes does not provide accurate data for fitting the α process of the quenched sample.

In addition, the decrease in the dielectric constant observed in Figure 2a at temperatures above 30°C implies that:

- (1) the crystallization process is slow enough to be followed dielectrically, and;
- (2) the crystallization process is taking place in this range of temperatures.

This is in good agreement with the d.s.c. measurements of the quenched sample, which showed that PHB exhibits an exothermic crystallization peak at 45°C (see Figure 1). Therefore, it would be of interest to follow the crystallization kinetics of amorphous PHB.

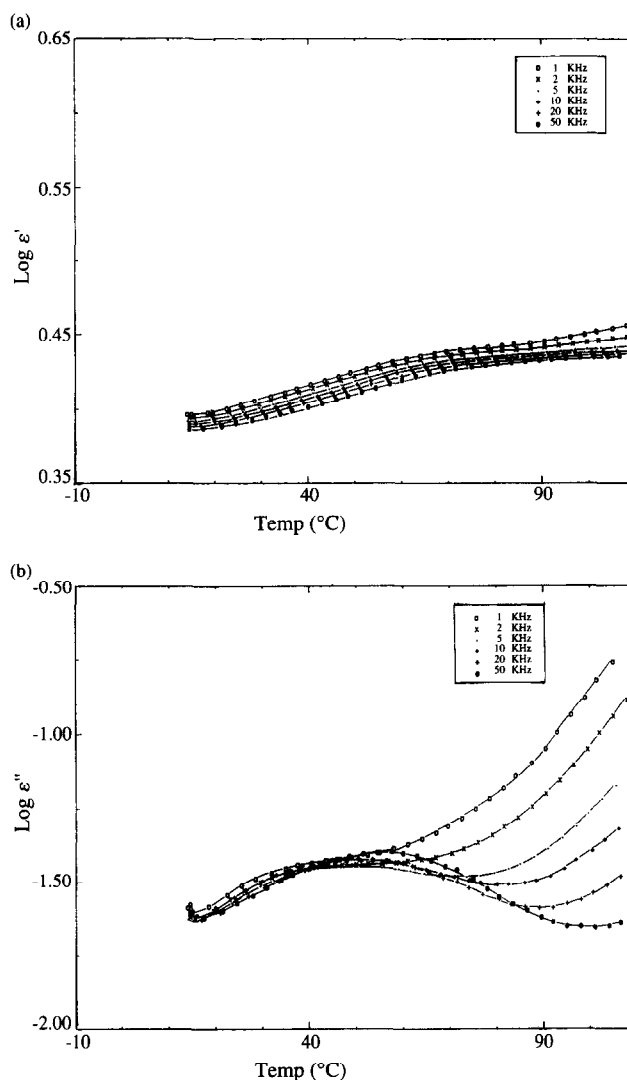


Figure 3 Temperature dependencies of (a) dielectric constant, ϵ' , and (b) dielectric loss, ϵ'' , at various frequencies for annealed PHB

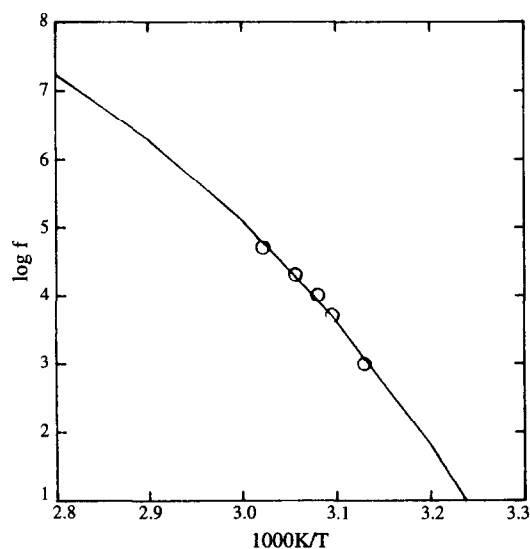


Figure 4 Activation diagram of the glass process for annealed PHB

However, a prerequisite for the study of the crystallization kinetics by the dielectric method is to trace the optimum crystallization temperature $T_{C(\text{max})}$, where each method of investigation (dielectric, d.s.c., optical, etc.) detects another molecular level²⁵. The term 'optimum

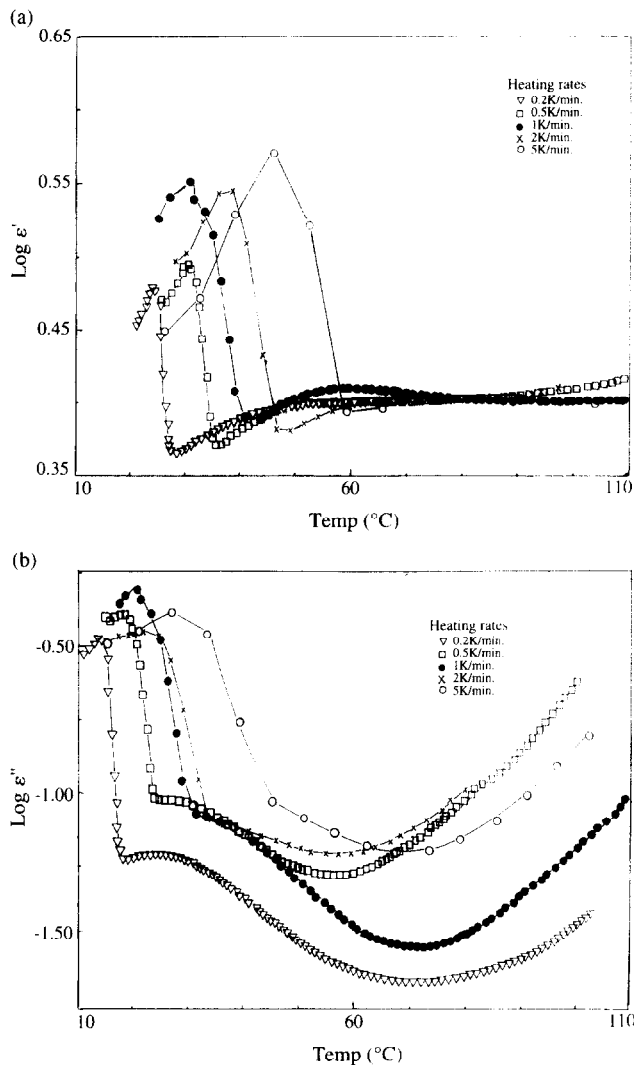


Figure 5 Temperature dependencies of (a) dielectric constant, ϵ' , and (b) dielectric loss, ϵ'' , at different heating rates for amorphous PHB at 10^4 Hz

crystallization temperature' is used to indicate the temperature at zero heating rate where large spherulites grow at a small rate of nucleation. Accordingly, the temperature dependence of ϵ' and ϵ'' at different heating rates (0.2, 1, 2 and 5°C min^{-1}) has been measured at 10^4 Hz and presented in Figure 5. It can be seen in Figure 5a that the expected increase in the dielectric constant with temperature is observed only at low temperatures. Thereafter, this increase is outweighed by the strong decrease caused by the crystallization process, which leads to a strong decrease in the number of freely reorienting dipoles. It can also be observed in this figure that the temperature at which the dielectric constant starts to decrease (i.e. when the crystallization process starts) is strongly dependent on the heating rate, where the higher the heating rate the higher is the onset temperature of crystallization T_{onset} . This finding implies that the crystallization kinetics is of the same order of magnitude as the rate from the measurements. The optimum crystallization temperature, $T_{\text{C(max)}}$, can be obtained by plotting the onset temperature of crystallization, T_{onset} , against the heating rate, as shown in Figure 6, and extrapolating T_{onset} to zero heating rate. The obtained value of the optimum crystallization temperature, $T_{\text{C(max)}}$, is about 25°C .

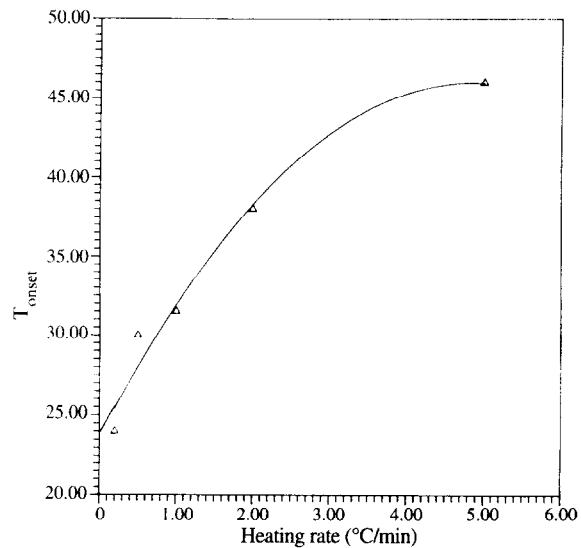


Figure 6 The onset crystallization temperature, T_{onset} , as a function of heating rate

On the other hand, the temperature dependence of dielectric loss presented in Figure 5b shows a relaxation process appearing at temperatures slightly higher than T_{onset} . This relaxation process is simply due to the α_a glass relaxation process of the constrained amorphous part, which is restricted within the spherulites (between crystalline lamellae).

Furthermore, it can be seen that the relaxation temperature, T_{max} , of the glass process is rate-dependent, where the higher the heating rate the higher is T_{max} . Moreover, the positions of the relaxation maxima are very close to those observed in annealed samples (see Figure 3). This finding implies that the higher the heating rate the greater are the constraints on the amorphous region and consequently the higher T_g . This result can be understood in view of the work done by Barham *et al.*^{16,17}, who showed that the rate of nucleation of PHB increases rapidly with increasing temperature, reaching its maximum value at 80°C then decreasing again. Also, they reported that the increase of the crystallization temperature from 20 to 40 and 80°C led to an increase in the nucleation rate constants by factors of 100 and 300, respectively. Therefore, one would expect that the higher the heating rate the shorter the time spent by the sample at lower temperatures, and consequently the number of nuclei (spherulites) formed at a high heating rate would be larger than that at slower heating rate, taking into consideration the following: (1) the spherulite growth rate increases by a factor of less than 10 upon increasing the temperature from 20 to 80°C , while the rate of nucleation increases by a factor of 300¹⁷; (2) the highest heating rate used in our study (0.083 K s^{-1}) is still lower than the smallest nucleation rate used by Barham *et al.* at 20°C ($0.1 \text{ events s}^{-1} \text{ mm}^{-3}$)¹⁶.

Accordingly, it can be concluded that the heating rate leads not only to a higher number of spherulites per unit volume but also to a smaller size of crystallites. The high population of small spherulites could restrict the whole cooperative motion responsible for the glass process. Therefore, these small spherulites could be envisaged to act as thermoreversible cross-links.

However, lower heating rates would lead to smaller numbers of large spherulites concentrated in a certain region. Consequently, it would be expected that the

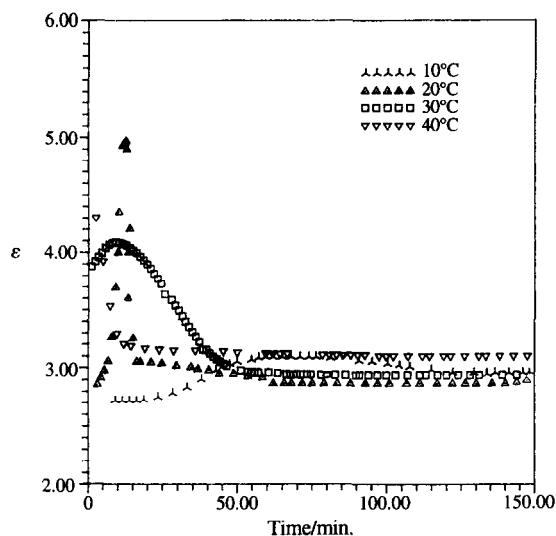


Figure 7 Dielectric constant, ϵ' , as a function of time at different crystallization temperatures (T_c)

restriction applied to the reorienting units will be concentrated in certain zones (crystalline and semi-crystalline), leaving the amorphous region less restricted than that obtained at higher heating rates.

On the other hand, the optimum crystallization temperature can be evaluated experimentally using the traditional method. This can be done by scanning the dielectric constant at different crystallization temperatures as a function of time, as shown in Figure 7. This figure shows that the dielectric constant increases during the first few minutes of measurement. The increase can be attributed either to an increase in the sample temperature to attain the measurement temperature (10, 20, 30 and 40°C), or to a global dipolar reorientation to attain a pre-ordered state that is required for achieving the crystallization process. However, due to the extremely small weight of the sample (0.2 g) which is placed between two copper electrodes (thermally conducting) and mounted in a preheated measuring cell with a cylindrical homogeneous heating flux, it is impossible to attribute this increase to the attainment of thermal equilibrium. This is because ϵ' increases for periods of time reaching 70 min for the isothermal temperature 10°C. Therefore, it can be concluded that this increase is mainly attributable to a pre-order reorientation process of the dipoles. This process is followed by the crystallization process which strongly restricts the dipolar reorientation and therefore leads to a rapid decrease in the dielectric constant (as observed in Figure 7). If one accepts this suggestion, it would be expected that the increase in the temperature would lead to a faster pre-order process, since the dipolar reorientation of the free dipoles of the amorphous phase will be faster by a factor of 200 for each 10°C increment (in this temperature range). This implies that the onset time at which the crystallization process starts will be shorter with increasing temperature. This has been already realized in Figure 7, where the onset crystallization time is shortened from 70 min to 14, 10 and 4 min for 10, 20, 30 and 40°C, respectively.

The decrease in the dielectric constant as a result of crystallization at a given temperature can be taken as an accurate measure for the amount of amorphous phase that has undergone crystallization, i.e. the increment in

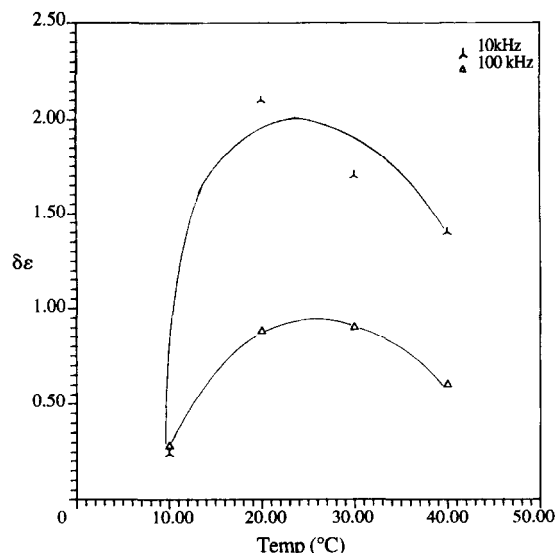


Figure 8 Decrement in the dielectric constant, $\delta\epsilon$, as a function of crystallization temperature (T_c) at 1064 Hz (Δ), and 10^5 Hz (\blacktriangledown) (see text)

the percentage of crystallinity. The key point in this approach is that the dipole relaxation is very specific to the local environment at a given temperature. A dipole in the amorphous phase can respond only to certain oscillation frequencies of the electric field. As the amorphous material crystallizes, there are fewer remaining amorphous dipoles able to respond to the field.

Accordingly, one would expect that a plot of the decrement in the dielectric constant, $\delta\epsilon$, would offer a possibility for determining the optimum crystallization temperature $T_{C(\max)}$, where $\delta\epsilon$ is the difference between the dielectric constant, ϵ' , at the onset time of crystallization and that after attaining equilibrium. Figure 8 shows that the optimum crystallization process is around 25°C for quenched PHB. This is in a good agreement with the results obtained by the above method (see Figure 6).

The results obtained from Figure 7 can also be employed to monitor the crystallization kinetics using Avrami relations^{26,27}. This can be done by using the normalized dielectric constant, ϵ_n , as a function of the crystallization time. The normalized dielectric constant is given by²⁸

$$\epsilon_n(t) = (\epsilon_i - \epsilon_t) / (\epsilon_i - \epsilon_f) \quad (2)$$

where ϵ_i is the dielectric constant at the start of crystallization, ϵ_f is the long-time limiting value and ϵ_t is the value at time t . Figure 9 is a representative example illustrating the variation of ϵ_n with time at 30°C. The normalized change in the dielectric constant is equivalent to the measurements of the relative degree of crystallinity. The time dependence of $\epsilon_n(t)$ can be described by the Avrami equation^{26,27}, using the following expression:

$$\epsilon_n(t) = 1 - \exp(-kt^n) \quad (3)$$

where k and n are the Avrami rate parameter and exponent, respectively.

The so called Avrami plot of $\log[-\ln(1 - \epsilon_n)]$ versus $\log(t)$ for the quenched PHB sample crystallized at 30°C and measured at 10^4 Hz is given in Figure 10. From the slope the Avrami exponent parameter of the main crystallization was found to be 3.8, which is consistent with sporadic three-dimensional spherulitic growth.

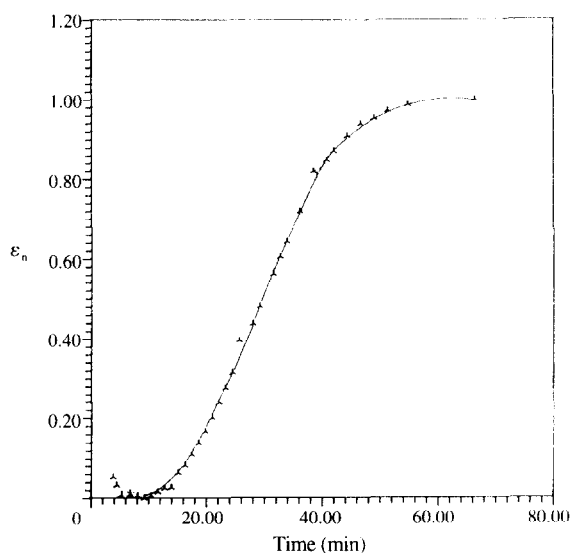


Figure 9 The normalized dielectric constant (ϵ_n) as a function of crystallization time at 10^4 Hz

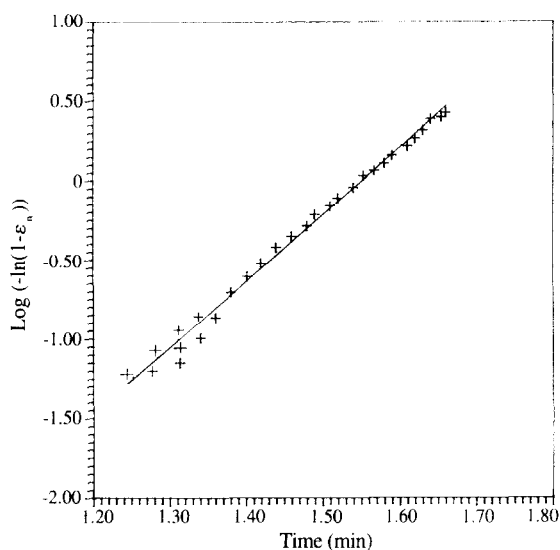


Figure 10 Avrami plot at $T_c = 30^\circ\text{C}$ and 10^4 Hz

Based on the above, it is clear that the dielectric measurements can supply some useful information about the crystallization kinetics and its parameters, where it was possible to fit the results using the Avrami equation.

It has been found that the optimum crystallization

temperature is about 25°C . In addition, the onset crystallization time is found to be temperature-dependent, and can be reduced to less than 5 min by annealing at 40°C . Furthermore, the dielectric measurements showed that the crystallization process reaches its end after about 1 h at the storage temperatures ($20\text{--}40^\circ\text{C}$)

REFERENCES

- Holmes, P. A., in *Developments in Crystalline Polymers*, Vol. 2, ed. D. C. Bassett. Elsevier, New York, 1988.
- Ranjana, S. and Alok, R. R. J. M. S., *Rev. Macromol. Chem.*, 1995, **C35**, 327.
- Bluhm, T. L., Hamer, G. K., Marchessault, R. H., Fyfe, C. A. and Veregin, R. P., *Macromolecules*, 1986, **19**, 2871.
- Kunioka, M., Tamaki, A. and Doi, Y., *Macromolecules*, 1989, **22**, 694.
- Bloembergen, S., Holden, D. A., Hamer, G. K., Bluhm, T. L. and Marchessault, R. H., *Macromolecules*, 1986, **19**, 2865.
- Marchessault, R. H., Bluhm, T. L., Deslandes, Y., Hamer, G. K., Orts, W. J., Sundararajan, P. R., Taylor, M. G., Bloembergen, S. and Holden, D. A., *Macromol. Chem., Macromol. Symp.*, 1988, **19**, 235.
- Fukuda, E. and Ando, Y., *Int. J. Biol. Macromol.*, 1986, **8**, 361.
- Mitomo, H., Barham, P. J. and Keller, A., *Polym. Commun.*, 1988, **29**, 112.
- Bauer, H. and Owen, A. J., *Colloid Polym. Sci.*, 1988, **266**, 241.
- Scandola, M., Pizzoli, M., Ceccorulli, G., Cesaro, A., Paoletti, S. and Navarini, L., *Int. J. Biol. Macromol.*, 1988, **10**, 373.
- Schlegel, H. G. and Steinbuchel, A. (ed.), *Proceedings of the International Symposium on Bacterial Polthydroxyalkanoates*. Goltze-Druck, Gottingen, 1993.
- Organ, S. J. and Barham, P. J., *Mater. Sci.*, 1991, **26**, 1368.
- Organ, S. J. and Barham, P. J., *Polymer*, 1993, **34**, 2169.
- Organ, S. J. and Barham, P. J., *Polymer*, 1993, **34**, 2175.
- Avella, M. and Martuscelli, E., *Polymer*, 1988, **29**, 1731.
- Barham, P. J., *J. Mater. Sci.*, 1984, **19**, 3826.
- Barham, P. J., Keller, A., Otun, E. L. and Holmes, P. J., *J. Mater. Sci.*, 1984, **19**, 2781.
- Howel, E. R., *Chem. Ind.*, 1982, 508.
- Cammenga, H. K., Eysel, W., Gmelin, E., Hemminger, W., Hohne, G. W. H. and Sarge, S. M., *Thermochim. Acta*, 1993, **219**, 333.
- Sarge, S., Gmelin, E., Hohne, G. W. H., Cammenga, H. K., Hemminger, W. and Eysel, W., *GEFTA*. University of Freiburg, Freiburg, 1994.
- Yokochi, M., Chatani, Y., Takdakoro, H., Teranishi, K. and Tani, H., *Polymer*, 1973, **14**, 267.
- Pechhold, W. and Stoll, B., *Polym. Bull.*, 1982, **7**, 413.
- Pechhold, W., Grassel, O. and von Soden, W., *Colloid Polym. Sci.*, 1990, **268**, 1089.
- Pechhold, W., Sautter, E., von Soden, W., Stoll, B. and Grassmann, H. P., *Macromol. Chem. Suppl.*, 1979, **3**, 247.
- Mansour, A. A., *Colloid Polym. Sci.*, 1995, **273**, 524.
- Avrami, M., *J. Chem. Phys.*, 1939, **7**, 1103.
- Avrami, M., *J. Chem. Phys.*, 1940, **8**, 212.
- D'Amore, A., Kenny, J. M. and Nicolais, L., *Polym. Eng. Sci.*, 1990, **30**, 314.